ARTICLE

Interfacial Self-Assembly of Metal-Mediated Viologen-Like Coordination Polyelectrolyte Hybrids of the Bisterpyridine Ligand and Their Optical, Electrochemical, and Electrochromic Properties

Chao-Feng Zhang,[†] An Liu,[†] Meng Chen,[†] Chikashi Nakamura,[‡] Jun Miyake,[‡] and Dong-Jin Qian*,[†]

Department of Chemistry, Fudan University, 220 Handan Road, Shanghai 200433, People's Republic of China, and Research Institute of Cell Engineering, AIST, Amagazaki 661-0974, Hyogo, Japan

ABSTRACT Metal-mediated coordination polyelectrolyte multilayers with a bisterpyridine ligand (Bisterpy) have been self-assembled at air−water interfaces via coordination reactions of the bidentate ligand Bisterpy with inorganic salts in the subphases. To avoid dissolution of the viologen-like coordination polyelectrolyte monolayers, anionic poly(styrenesulfonic acid-*o*-maleic) (PSS) acid was added in the subphases as a supporting layer. The average molecular area of the ligand Bisterpy could reach 1.2−1.5 nm^2 on the surfaces of the subphases containing mixtures of inorganic salts (M) and PSS, although the ligand was unable to form a stable monolayer on the pure water surface. The Langmuir−Blodgett (LB) method was used to deposit the Bisterpy/PSS and M-Bisterpy/PSS hybrid multilayers on the substrate surfaces, which were characterized by using absorption and fluorescence spectroscopy as well as electrochemical analysis. Quasi-reversible redox waves were recorded and centered at about −0.68 and −0.92 V (vs Ag/AgCl), respectively, corresponding to the two-electron process of the ligand, $Bisterpy^{2+} \leftrightarrow Bisterpy^{\bullet+} \leftrightarrow Bisterpy^{0}$, which were slightly shifted to lower potentials in the LB films of metal-mediated coordination polymers. The film compositions were determined by using X-ray photoelectron spectroscopy. The as-prepared LB films showed strong stability and good electrochromic response upon the applied potential of −1.1 V vs Ag/AgCl and thus could act as potential materials in the development of redox-based molecular switches and display devices.

KEYWORDS: interfacial assembly • coordination polyelectrolyte • Langmuir−Blodgett film • electrochemistry • electrochromic effect

INTRODUCTION

Coordination polymers have been recently attracted great interest with regard to the design and fabrication of novel materials and molecular devices (1). These well-defined, layered, organic−inorganic hybrids have a particularly attractive supramolecular structure and thus have been considered as potential materials in the construction of extended π-systems for organic semiconductors, optical and electrochemical molecular materials, and molecular-sized boxes or networks with channels or nanoporous cavities for selective molecular recognition and catalysts (2, 3). Generally, coordination polymers are prepared by coordination reactions between the multitopic ligands and transition-metal ions (4). On the basis of the coordinative features of the metal ions and ligands (bidentate, tridentate, and tetradentate), a large number of coordination polymers with unique structural features have been synthesized in solutions, and some of them have been immobilized or assembled on the substrate surfaces (5−8).

We are currently interested in the interfacial self-assembly of organized ultrathin films of coordination polymers, their nanocrystals, and supramolecular building blocks by using the Langmuir−Blodgett (LB), self-assembly, and layer-by-layer methods (9). These methods provide facile routes to the design of three-dimensional organized building blocks based on the structural features of transition-metal ions and ligands, as well as on the desired functions of the products (10). Because the multidentate ligands are connected by metal ions via a coordination bond, the as-prepared coordination polymers have great thermal, chemical, and structural stability as well as structural regularity and controllability, the features of which result in the molecular aggregates of coordination polymers being attractive supramolecular and nanostructural materials in practical applications for the development of molecular devices and machines.

The multitopic ligand 4′-(4-pyridyl)-2,2′:6′,2″-terpyridine (pyterpy, Figure 1a) contains one widely used 2,2′:6′,2″-terpyridine (terpy) coordinative site and another pyridyl site

* To whom correspondence should be addressed. E-mail: djqian@fudan.edu.cn. Tel/Fax: 86-21-65643666.
Received for review March 3, 2009 and accepted May 24, 2009
[†] Fudan University.
[‡] AIST.
DOI: 10.1021/am900135g

Published on Web 06/04/2009

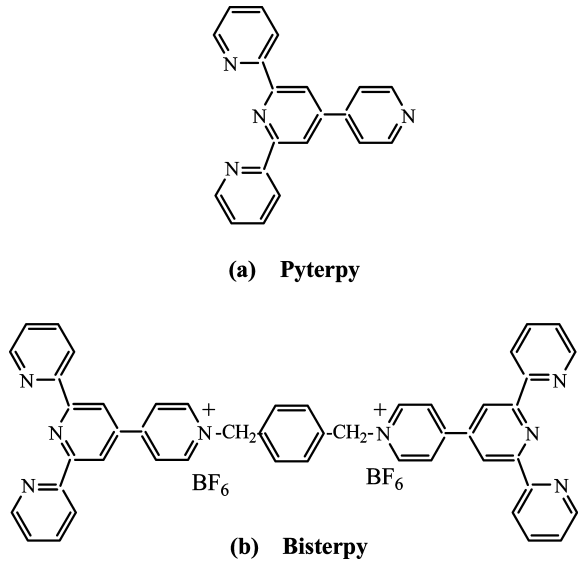

FIGURE 1. Bidentate ligands used in the present work.

at the 4′-position; these two sites are able to bind with different metal ions, thus leading to coordination polymers with various frameworks (11, 12). Moreover, the pyridyl site can react with organic halides to form N-alkylated pyterpy derivatives, which can react with a great number of transition-metal ions, including Fe^{2+}, $Ru^{2+/3+}$, Zn^{2+}, and Co^{2+}, to form viologen-like compounds or organic–inorganic hybrids (13). Kurth et al. recently found that, when pyterpy reacted with α,α′-dibromo-*p*-xylol, a new "bidentate-like" multitopic ligand of bisterpyridine (Bisterpy, Figure 1b), 2,2′:4′,4″-terpyridinium, 1″,1‴″-[1,4-phenylenebis(methylene)]bis[6′-(2-pyridinyl) bis[hexafluorophosphate(1−)], could be obtained (14). This ligand could coordinate with transition-metal ions to produce viologen-like polyelectrolytes with interesting electronic, optical, and magnetic properties (15, 16). By using the electrostatic layer-by-layer (LBL) self-assembly method, electrochromic multilayers of the viologen-like polyelectrolytes with anionic polymers have been constructed.

In the present work, several viologen-like coordination polymers of metal–Bisterpy (M-Bisterpy) have been assembled at the air–water interface, on the basis of an interfacial coordination reaction of inorganic ions and Bisterpy. It was found that, although the ligand Bisterpy was unable to form stable monolayers on the pure water and inorganic salt subphase surfaces, it could be stabilized on subphase surfaces containing a small amount of the anionic polyelectrolyte of poly(styrenesulfonic acid-*o*-maleic) (PSS) acid. When mixtures of inorganic salts and PSS were used as subphases, stable monolayers of M-Bisterpy coordination polymeric hybrids could form and be transferred onto substrate surfaces by using the LB method, which provided not only a facile route to prepare organized ultrathin films but also a route to study interfacial interactions between floating molecules and species in the subphases. Generally, water-soluble electrolytes or polyelectrolytes have been unable to form stable monolayers at the air–water interfaces; here with the use of oppositely charged polyelectrolyte and inorganic salts as subphases, Bisterpy was stabilized on the water surface and formed hybrid monolayers. The

Table 1. Subphase Compositions and Average Bisterpy Molecular Areas for the Monolayers and LB Films Prepared in the Present Work

monolayer/LB film	subphase	area of Bisterpy (nm^2)
Bisterpy/PSS	0.01 mg/mL PSS	0.79
Zn-Bisterpy/PSS	1 mM $ZnSO_4$ and 0.01 mg/mL PSS	1.21
Cd-Bisterpy/PSS	1 mM $CdCl_2$ and 0.01 mg/mL PSS	1.42
Fe-Bisterpy/PSS	1 mM $Fe(BF_4)_2$ and 0.01 mg/mL PSS	1.51

prepared LB films of M-Bisterpy coordination polymers were characterized by using UV–vis absorption, fluorescence, X-ray diffraction (XRD), and X-ray photoelectron spectra (XPS). Cyclic voltammogram studies revealed two couples of quasi-reversible redox waves corresponding to the two-electron process of the ligand both in solutions and in LB films. Some immobilized films of the coordination polymers showed good electrochromic response upon an applied potential of −1.1 V vs Ag/AgCl. Thus, the present methodology could provide a facile route for the fabrication of condensed and organized thin films of Bisterpy and its metal-mediated coordination polymers, which could be developed as molecular materials for redox-based molecular switches and display devices.

EXPERIMENTAL SECTION

Materials. 2-Acetylpyridine, pyridine-4-carbaldehyde, α,α′-dibromo-*p*-xylene (97%), and iron(II) tetrafluoroborate hexahydrate (97%) were purchased from Acros Organics. Ammonium chloride, $ZnSO_4$, $CdCl_2$ and methanol were obtained from Shanghai Chemical Reagent Co. Chloroform and methanol used as spreading solvents were purchased from Fisher Chemicals Co. Poly(styrenesulfonic acid-*o*-maleic) acid was obtained from Aldrich Chemical Co. All chemicals were used as received without further purification. Double-distilled water (first deionized) was used to prepare aqueous solutions.

The ligand 4′-(4-pyridyl)-2,2′:6′,2″-terpyridine (Pyterpy) and the "bidentate-like" multitopic ligand of Bisterpy were synthesized according to literature methods with slight modifications for Bisterpy (11, 12). Briefly, for the synthesis of Bisterpy, 5 mmol of α,α′-dibromo-*p*-xylene and 10 mmol of pyterpy were refluxed in acetonitrile for 10 h. The yellow precipitate was collected and then dissolved in a small amount of water, followed by addition of an aqueous solution of 0.35 M NH_4PF_6. The precipitate was filtered, washed with copious amounts of water and ethanol, and dried at room temperature and was then characterized by ^1H NMR and elemental analysis. ^1H NMR (CD_3CN, ppm): δ 8.78 (4H), 8.61 (4H), 8.49 (4H), 8.48 (4H), 8.46 (4H), 7.82 (4H), 7.40 (4H), 7.31 (4H), 5.62 (4H). Anal. Calcd for $C_{48}H_{36}N_8P_2F_{12}\cdot 4H_2O$: C, 52.99; H, 4.05; N, 10.31. Found: C, 53.16; H, 3.94; N, 10.25.

Preparation of Metal–Bisterpy Coordination Polymers at Interfaces. Monolayers of the ligand Bisterpy and its metal-mediated coordination polymers of M-Bisterpy were prepared by spreading a dilute (~5×10^{-5} mol/L) Bisterpy solution in mixed solvents of chloroform and methanol (ratio 4:1, v/v) onto surfaces of the subphases of pure water, inorganic salts, PSS, and mixtures of PSS with inorganic salts. Details of the subphases used are summarized in Table 1. The surface pressure–area (π–A) and area–time (A–t) isotherm measurements as well as LB film transfers were performed using a KSV 5000 minitrough (KSV Instrument Co., Finland) operated at a continuous speed for two barriers of 10 cm^2/min at 20 °C. The accuracy of the surface-pressure measurement was 0.01 mN/m.

Transfer of the monolayers of the ligand Bisterpy and M-Bisterpy coordination polymers onto solid plates was done by a vertical dipping method at 20 mN/m. For every transfer, the dipping speed was 2 mm/min.

Measurements. The UV−vis absorption spectra of the transferred LB films were measured using a Shimadzu UV-1601 UV−vis spectrophotometer. Fluorescence spectra were recorded by using a Shimadzu RF-5300PC spectrophotometer.

XPS spectra for the LB films on the quartz substrate surfaces were recorded using a VGESCALAB MKII multifunction spectrometer, with non-monochromated Mg Kα X-rays as the excitation source. The system was carefully calibrated by the Fermi edge of nickel, Au $4f_{2/7}$, and Cu $2p_{2/3}$ binding energies. A pass energy of 70 eV and step size of 1 eV were chosen when taking spectra. In the analysis chamber pressures of $(1-2) \times 10^{-7}$ Pa were routinely maintained. The binding energies obtained in the XPS analysis were corrected by referencing the C1s peak to 284.60 eV. X-ray diffraction for the LB films on the quartz substrate surface was carried out with a Rigaku D/max-γB diffractometry in transition mode and Cu Kα radiation. The scan range of 2θ was 1−50° with a step interval of 0.02°.

Transmission electron microscope images were taken on a Hitachi H-600 electron microscope operating at 75 kV. Monolayers of the Bisterpy/PSS and Zn-Bisterpy/PSS coordination polymers were deposited on 230 mesh copper grid covered with formvar at 20 mN/m.

Electrochemistry. The cyclic voltammogram (CV) for the multilayers of Bisterpy/PSS and M-Bisterpy/PSS coordination polymers was measured by using an electrochemical analyzer (CHI 601b). A Pt wire and Ag/AgCl electrode were used as the auxiliary and reference electrodes, respectively, and an indium−tin oxide (ITO) electrode, coated with the multilayers, was used as the working electrode with 10 mM KCl as the electrolyte. An initial potential of 0 or 0.8 V was applied for 2 s, and subsequent cyclic scans to a final potential of −1.2 V were done for 10 cycles. The CV curves and data reported in the present work were the 10th cycle.

The electrochromic experiments were performed by using the three-electrode system above in a transparent quartz cell for the UV−vis absorption measurements under a given applied potential of −1.1 V (vs Ag/AgCl) in the 10 mM KCl electrolyte solution. The photos of color change for the LB films on ITO electrodes were taken by a commonly used camera upon the applied potential or not. All electrochemical measurements were done under an Ar atmosphere at room temperature.

RESULTS AND DISCUSSION

In the previous work of Kurth and co-workers, a ligand of $BisterpyBr_2$ was synthesized (14); here the anionic counterion of Br^- was replaced by PF_6^- on the basis of the following considerations. (1) The water solubility was decreased when $BisterpyBr_2$ was changed to $Bisterpy(PF_6)_2$, which was beneficial for the formation of insoluble monolayers of Bisterpy. (2) The replacement of anionic X^- ions by the larger PF_6^- has been often used to purify a great number of cationic organic salts, such as viologen derivatives (17). After reprecipitation from an aqueous solution of $BisterpyBr_2$ in 0.35 M NH_4PF_6, the pure pale product of $Bisterpy(PF_6)_2$ could be obtained without further purification. For simplicity, the abbreviation of Bisterpy is used instead of $Bisterpy(PF_6)_2$ in the following sections.

Monolayer Behaviors of the Ligand Bisterpy. Since Bisterpy is a cationic ligand with two bidentate terpy coordination sites, its interfacial behaviors are expected to be largely dependent on the subphase conditions, especially the subphase compositions, which provide the possibility of preparing monomolecular films of coordination polymers at interfaces. Thus, we first measured the monolayer behaviors of the Bisterpy ligand on the surfaces of subphases containing several transition-metal ions and an anionic polyelectrolyte.

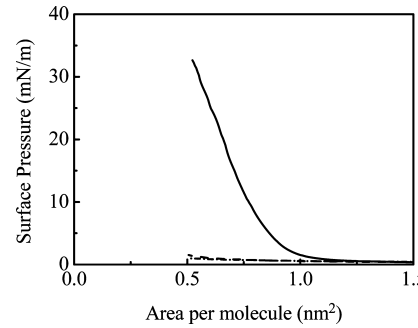

FIGURE 2. $\pi-A$ isotherms for monolayers of Bisterpy on pure water (- - -), 1 mM $ZnSO_4$ (- · - ·), and 0.01 mg/mL PSS (—) subphase surfaces.

Figure 2 shows the $\pi-A$ isotherms for the monolayers of ligand Bisterpy on the pure water, 1 mmol/L $ZnSO_4$, and 0.01 mg/mL PSS subphase surfaces. Almost no increase of surface pressure was recorded for the ligand Bisterpy on the pure water and 1 mmol/L $ZnSO_4$ subphase surfaces, indicating that Bisterpy was unable to form a stable monomolecular layer in both cases. During experiments, we found that even the concentrations of $ZnSO_4$ largely increased (up to 1 mol/L); stable monolayers of Bisterpy were still unable to form. When other inorganic salts of $CdCl_2$ or $Fe(BF_4)_2$ were used as the subphases, stable monolayers also failed to form. These may be ascribed to the fact that (i) the ligand Bisterpy could slightly dissolve and (ii) its M-Bisterpy complexes could easily dissolve into water, resulting in a difficulty to form their insoluble monomolecular layers at the air−water interface.

However, when the ligand Bisterpy was spread on the surface of a subphase containing 0.01 mg/mL of the anionic polymer PSS, the surface pressure greatly increased to over 30 mN/m after compression. The average molecular area of Bisterpy could reach about 0.79 nm^2 per molecule of Bisterpy. The enhanced surface pressure and enlarged molecular area indicated that PSS could prevent the ligand Bisterpy from dissolving into the water phase and support the formation of a Bisterpy monolayer, which may be due to a strong electrostatic interaction between Bisterpy and PSS. The produced Bisterpy/PSS hybrid was hardly soluble into water and floated at the air−water interface. This kind of monolayer formation method has been often used for the preparation of monolayers of polyelectrolytes and proteins. For instance, it has been previously revealed that positively charged poly-L-lysine or $CaCl_2$ in subphases could stabilize the monolayer formation of hydrogenase (18). PSS has also often been used as an alternative layer for the preparation of LB films of charged species or layer-by-layer (LBL) multilayers of proteins and viologen polyelectrolytes (19).

When the ligand Bisterpy was spread on subphase surfaces containing mixtures of PSS and inorganic salts, both

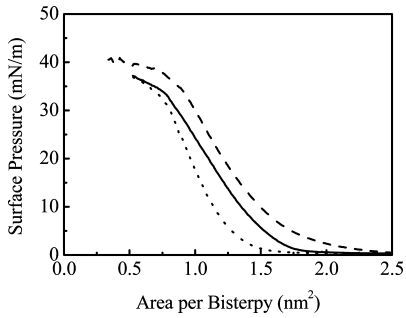

FIGURE 3. $\pi-A$ isotherms for the monolayers of Bisterpy on the surfaces of the subphases of $CdCl_2$-PSS (—), $Fe(BF_4)_2$-PSS (- - -) and $ZnSO_4$−PSS (· · ·).

collapsed surface pressures and average molecular area of Bisterpy increased greatly. Figure 3 shows the $\pi-A$ isotherms for the monolayers of Bisterpy on mixtures of 1 mmol/L inorganic salts and 0.01 mg/mL PSS subphase surfaces at room temperature. The highest surface pressure increased up to about 40 mN/m, with the average occupied molecular area of Bisterpy falling in the range of 1.2−1.5 nm^2. We have previously reported that $ZnSO_4$ could react with Pyterpy to form its metalated complex $Zn(Pyterpy)_2$, on the basis of the coordination interaction of Zn^{2+} with the terpy site of the ligand Pyterpy (20). Thus, the increased average molecular area for the Bisterpy monolayer on the PSS-$ZnSO_4$ subphase surfaces could be attributed to a reorganization of Bisterpy at the interface because of the coordination reaction of Zn^{2+} ions with Bisterpy, which resulted in the formation of a Zn^{2+}-Bisterpy coordination polymer. The produced coordination polymer was a positively charged polyelectrolyte, which could electrostatically interact with the anionic polymer of PSS in the subphases, stabilizing its monolayer at the air−water interface, due to the formation of an insoluble Zn^{2+}-Bisterpy/PSS hybrid.

It has been revealed that the ligand Bisterpy could react with various transition-metal ions (Ms); on the basis of the coordination reaction of M-terpy, we further investigated its monolayer behaviors on the surfaces of subphases containing mixtures of PSS and $CdCl_2$ or $Fe(BF_4)_2$. As shown in Figure 3, similar $\pi-A$ isotherms of Bisterpy were recorded in all cases. The average molecular areas for Bisterpy on these subphase surfaces are calculated and summarized in Table 1. On the basis of the model structure of M-Pyterpy metalated complexes (21), the molecular area of M-Bisterpy was estimated to be about 1.8 nm^2, slightly larger than the value we obtained from the $\pi-A$ isotherms. Possible reasons may be ascribed to the solubilities of the polyelectrolyte products, but the data were comparable. Thus, we concluded that M-Bisterpy coordination polymers were formed and stabilized at the interfaces due to the interfacial coordination reaction between metal ions and Bisterpy, as well as to the electrostatic interaction between the positively charged viologen-like polyelectrolytes and the anionic polymer of PSS (Scheme 1).

As the collapsed surface pressures were not as high (30−40 mN/m) as those displayed by the traditional amphiphiles, we measured the $A-t$ isotherms for the monolayers of Bisterpy and its coordination polymers to reveal the monolayer stability. Figure S1 (Supporting Information) shows the $A-t$ curves for the Bisterpy and Zn-Bisterpy monolayers, which revealed a very small decrease (below 0.05 nm^2) of the molecular occupied area after 2 h when the surface pressure was kept at 20 mN/m. The results suggested that these monolayers were very stable even though both Bisterpy and its coordination polymers are not traditional amphiphiles.

Langmuir−Blodgett Films of Bisterpy/PSS and M-Bisterpy/PSS Hybrids. Monolayers of Bisterpy and its metal-mediated coordination polymers on the PSS subphase surfaces were transferred onto substrate surfaces by the traditional vertical dipping method at 20 mN/m. The transfer ratio indicated that the Z-type of LB films was deposited. These monolayers could also be transferred by the horizontal lifting technique when a hydrophobic substrate was used. The as-prepared LB films were characterized by using UV−vis absorption, fluorescence, and X-ray photoelectron spectra as well as electrochemical analysis.

Scheme 1. Schematic Drawing for the Self-Assembly of M-Bisterpy/PSS Coordination Polyelectrolyte Hybrids at Air−Water Interfaces

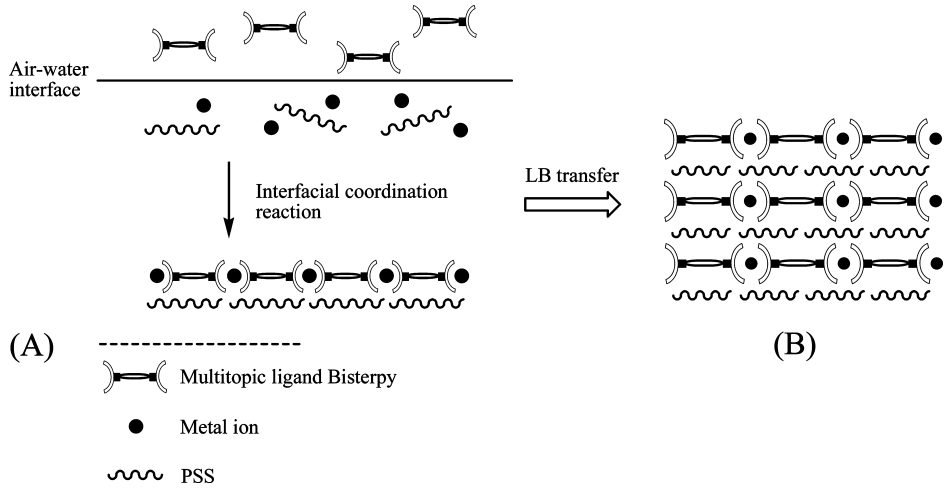

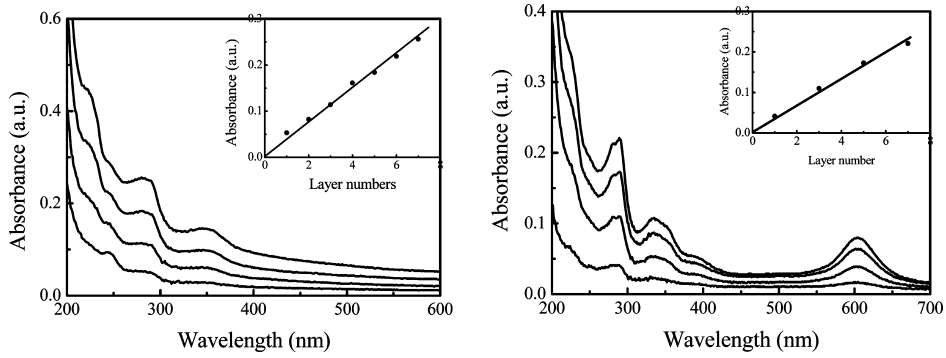

FIGURE 4. Absorption spectra for the LB films of (A. left) Bisterpy/PSS and (B, right) Fe-Bisterpy/PSS hybrids. Inset: plots of absorption intensity vs number of layers of the LB films transferred.

Absorbance. UV−vis absorption spectra were measured for the LB films of Bisterpy/PSS and M-Bisterpy/PSS after deposition. As examples, Figure 4 shows the absorption curves for one to seven layers for the LB films of Zn-Bisterpy/PSS and Fe-Bisterpy/PSS, respectively; the inserts give plots of absorption intensity vs the number of layers deposited. It could be seen that all spectra were composed of several peaks in the range 240−360 nm, which were attributed to ligand-based $\pi-\pi^*$ and $n-\pi^*$ transitions (11). For the LB film of Fe-Bisterpy/PSS, in addition to the peaks at about 241, 277, and 320 nm, there was another peak at around 600 nm, which was ascribed to its metal-to-ligand charge-transfer (MLCT) band (11).

A linear increase of the absorption intensity with the number of layers for both LB films was recorded, as shown by the insets in Figure 4, indicating that similar amounts of M-Bisterpy coordination polymers were transferred during each LB film deposition. Previously, we have prepared several kinds of LB films of other metal-mediated coordination polymers and multiporphyrin arrays (22), but usually Z-type LB films were deposited with a poor transfer ratio after several times of deposition. Here, we could have a good monolayer transfer for a great number of layers. This difference may be attributed to the coexisting negatively charged PSS polyelectrolyte, which was adsorbed by the positively charged M-Bisterpy layer and then formed closely packed three-dimensional condensed films of M-Bisterpy/PSS hybrids due to interlayer electrostatic interaction.

Luminescence. We have previously found that the ligand Pyterpy could give off rather strong yellow light under UV radiation (emission wavelength at 364 nm) (16). After it reacted with α,α′-dibromo-*p*-xylol, the product of Bisterpy gave off blue luminescent emission at around 454 nm (Figure 5A). When a given amount of $ZnSO_4$ was added to the dilute solution of Bisterpy, the fluorescence emission appeared at about 412 nm (Figure 5B), which could be attributed to the emission of a Zn-Bisterpy metalated complex.

However, almost no fluorescent emission was recorded for the LB films of either Bisterpy/PSS or M-Bisterpy/PSS. It has been revealed that, for the Fe-Bisterpy coordination polymer, this phenomenon could be ascribed to the fact that the fluorescence was quenched by Fe^{2+} ions, as we have observed for their Pyterpy complexes (16). To clarify why

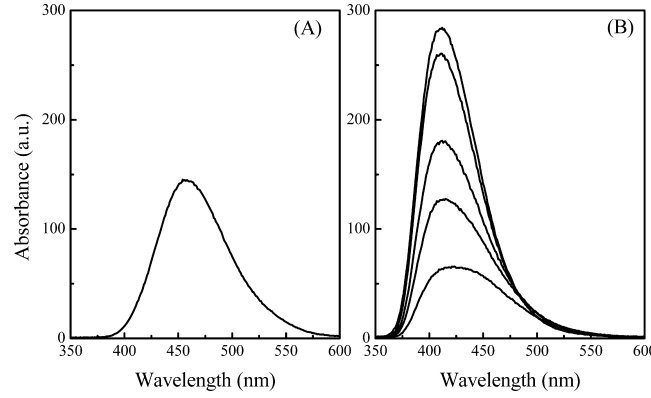

FIGURE 5. Fluorescence spectra for (A) Bisterpy in methanol solution and (B) mixtures of Zn-Bisterpy and PSS in molar ratios of 1:0 to 1:10 (top to bottom).

no fluorescence emission was recorded for the other LB films of Bisterpy/PSS and Zn(Cd)-Bisterpy/PSS, we investigated the emission spectra for the pure Bisterpy ligand and its mixtures with $ZnSO_4$ and $CdCl_2$ in the presence of different amounts of PSS in methanol solutions.

As an example, Figure 5B shows the emission spectra for the Zn-Bisterpy complex in the presence of different molar ratios of PSS. These curves indicated that, during the addition of the anionic polyelectrolyte PSS in the mixtures, the emissions from the Zn-Bisterpy complex was decreased; that is, PSS could quench the emissions from the Zn-Bisterpy complex. Similar fluorescence quenching was also observed for the pure ligand and Cd-Bisterpy complex when PSS was added. Hence, we concluded that the significant luminescent quench in the prepared LB films of both the Bisterpy ligand and its Zn(Cd)-coordination polymer hybrids was because of the coexisting anionic polymer of PSS.

X-ray Photoelectron Spectra. Element compositions for the LB films prepared were detected by using XPS spectra, which showed several peaks in the binding energy from 190 to 1100 eV (spectra are shown in the Supporting Information, Figure S2). The binding energy for each peak is summarized in Table 2. Except for the Si and O elements (partly) from the quartz substrate, four or five elements were detected from the LB films of Bisterpy/PSS or M-Bisterpy/PSS, respectively.

In detail, the Bisterpy/PSS LB film was composed of S(2p), C(1s), N(1s) and O(1s) elements, among which C (partly) and N were from the ligand of Bisterpy, while S, C (partly), and

Table 2. Deconvolution of XPS Peaks

LB film	S(2p)	C(1s)	N(1s)	O(1s)	M(2p/3d)
Zn-Bisterpy/PSS	168.2	284.8	399.8	532.5	1022.3 (Zn(2p))
Cd-Bisterpy/PSS	168.2	284.8	400.5	532.5	406.0, 413.0 (Cd(3d))
Fe-Bisterpy/PSS	167.6	284.8	400.1	532.6	705.8 (Fe(2p))
Bisterpy/PSS	167.3	284.8	396.2	532.4	

O (partly) were from the anionic polymer of PSS. On the other hand, the M-Bisterpy/PSS LB films were composed of the above four elements as well as the corresponding metal element (Zn^{2+}, Cd^{2+}, or Fe^{2+}), which was from the connector of the inorganic salts. These data confirmed that (1) PSS was adsorbed by the Bisterpy monolayer and coexisted in the LB films and (2) the metal ions were coordinated with the Bisterpy ligands and formed coordination polymers at interfaces. It is noted that no XPS peaks corresponding to the smaller anionic ions from inorganic salts such as BF_4^- and PF_6^- were detected, which could be attributed to the fact that the smaller anionic ions were replaced by the larger anionic polymer of PSS during the formation of the monolayers and LB films of Bisterpy/PSS and M-Bisterpy/PSS.

From the XPS data, it was found that the elemental ratios N:Fe and N:Zn were in the range of 5.6−8.4 for the LB films of Fe-Bisterpy/PSS and Zn-Bisterpy/PSS (23). These data confirmed the formation of M-Bisterpy coordination polymers, because the elemental ratio N:M was 8 when the coordination polymer was formed with one metal ion and one ligand. If the polymerization did not take place, the following two kinds of simple metalated complexes should be formed: that is, $M(Bisterpy)_2X_2$ and $M_2(Bisterpy)X_4$ (X is the counterion). The N:M elemental ratios for the complexes of $M(Bisterpy)_2X_2$ and $M_2(Bisterpy)X_4$ were 16 and 4, respectively (one ligand of Bisterpy contains eight nitrogen atoms).

The XRD measurements showed one broad band with 2θ at about 20° for either the Bisterpy/PSS or M-Bisterpy/PSS LB films, which corresponded to a layer space of about 4.4 Å. This small layer space may indicate a closely packed arrangement of M-Bisterpy and PSS due to the electrostatic interaction. More experiments with the use of other anionic polymers or inserted amphiphiles in the monolayers are under consideration to clarify the layered structure of the present coordination polymer LB films.

On the basis of the $\pi-A$ isotherms, XPS, absorption, and fluorescence spectral features discussed above, the crystal structure of the $M(Pyterpy)_2[BF_4]_2$ metalated complexes, and the structure of the metal-mediated coordination polymers reported in the literature (11b, 22c, 24), we proposed a schematic model for the present M-Bisterpy coordination polyelectrolyte formed at the interfaces. As shown in Scheme 1A, each metal ion coordinated with two 2,2′:6′,2″-terpyridine sites of the ligand Bisterpy to form a six-coordinate metal ion center. Monolayers of these coordination polyelectrolytes were stabilized on the PSS subphase surfaces. During the LB film transfer, alternative multilayers of organic−inorganic hybrids composed of M-Bisterpy complexes and PSS were obtained, as shown in Scheme 1B.

Transmission Electron Microscopy. Surface morphologies for the LB films of Bisterpy/PSS and M-Bisterpy/PSS were investigated by using TEM. As an example, Figure 6 shows the TEM images of Bisterpy/PSS and Zn-Bisterpy/PSS deposited at 20 mN/m. These photos confirmed that the Bisterpy ligand and its coordination polymeric hybrids formed uniform films at interfaces. During experiments, we further found that some areas formed a bilayer- or wrinkle-like structure (as inserted in Figure 6) when the monolayers were compressed to about 30 mN/m (nearly collapsed). This may be attributed to the fact that the monolayers were wrinkled with compression because Bisterpy and its coordination polymers were not traditional amphiphiles with a weaker intralayer hydrophobic interaction.

Electrochemistry. Since the Bisterpy ligand and its metalated complexes are electroactive materials with unique electrochromic properties, an investigation of their electrochemical properties in the LB films is important for the development of novel molecular materials and devices. In the present work, the cyclic voltammetric behaviors of the pure Bisterpy and its coordination polymers in the LB films were described. As control experiments, we also measured the CVs for the pure ligand and its metalated complexes in casting films or in solutions. Since the Bisterpy ligand was only slightly soluble in water, we prepared its casting film on a glassy-carbon (GC) electrode surface for the CV measurements. The results indicated that similar redox waves were recorded for the Bisterpy and Zn(Cd)-Bisterpy complexes in either solutions or LB films, with slightly different waves being obtained for the Fe-Bisterpy complex as described below.

Figure 7 shows the CV curves for the ITO electrodes modified by the ligand Bisterpy and Bisterpy/PSS LB films in the 10 mmol/L KCl electrolyte solution at a scan rate of 50 mV/s. The CV curve in Figure 7A was prepared from a casting film of Bisterpy on the GC electrode, which revealed two couples of redox waves at potentials of −0.45 and −0.82 V during the cathodic sweep, as well as at −1.1 and −0.75 V during the anionic sweep, respectively. These were ascribed to the two-electron process of the ligand Bisterpy, that is, $Bisterpy^{2+} \leftrightarrow Bisterpy^{\bullet+} \leftrightarrow Bisterpy^0$, just as those of the positively charged viologen derivatives (Vs) ($V^{2+} \leftrightarrow V^{\bullet+} \leftrightarrow V^0$) (25). These two couples of redox waves remained in the CV curve of the Bisterpy/PSS LB film as shown in Figure 7B, but their relative intensity changed a great deal; the relative intensity of the first couple became a great deal weaker than that of the second couple.

Figures 8A and 9A show the CV curves for the clean ITO electrodes immersed in the 10 mM KCl electrolyte solution containing Zn-Bisterpy and Fe-Bisterpy metalated complexes at a scan rate of 50 mV/s, respectively. Similar to the curves observed for the pure ligand casting film, two couples of redox waves were recorded for the Zn-Bisterpy complex in solution, which were attributed to the two-electron process of the ligand, $Bisterpy^{2+} \leftrightarrow Bisterpy^{\bullet+} \leftrightarrow Bisterpy^0$. For the Fe-Bisterpy complex, in addition to the two redox waves of Bisterpy appearing at about −0.71/−0.84 and −0.86/−1.11 V, the same as those for the pure ligand and Zn-Bisterpy complex above, another pair of redox waves appeared at

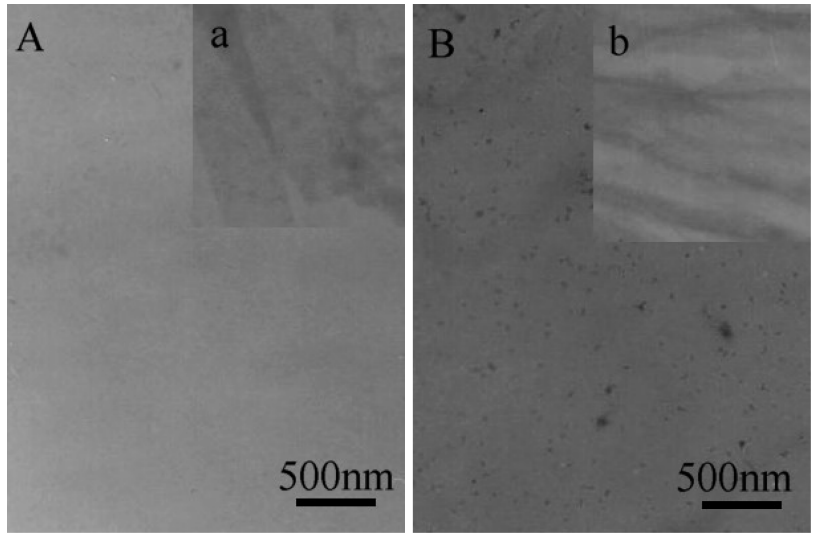

FIGURE 6. TEM images for the LB films of (A) Bisterpy/PSS and (B) Zn-Bisterpy/PSS deposited at 20 mN/m. Inserts a and b show films deposited at around 30 mN/m.

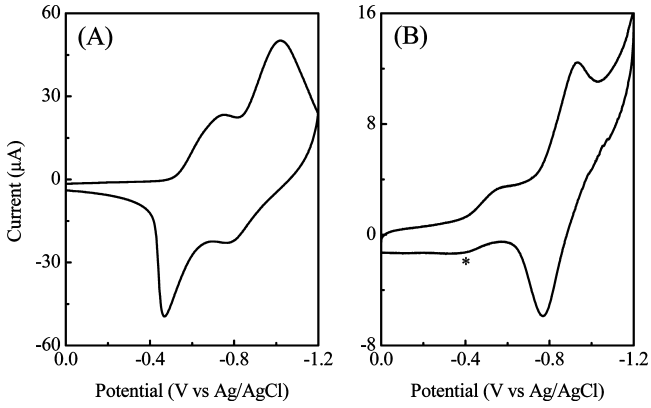

FIGURE 7. Cyclic voltammograms for (A) Bisterpy casting film on a glassy-carbon electrode and (B) a Bisterpy/PSS LB film modified electrode in the 10 mmol/L KCl electrolyte solution at scan rate of 50 mV/s. (the asterisk refers to the first cathodic peak position).

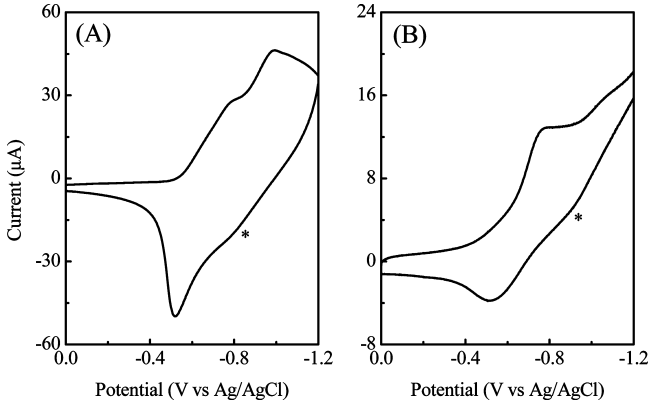

FIGURE 8. Cyclic voltammograms for (A) the Zn-Bisterpy complex and (B) the Zn-Bisterpy/PSS LB film in the 10 mmol/L KCl electrolyte solution at a scan rate of 50 mV/s (the asterisk refers to the second cathodic peak position).

about −0.05/−0.41 V, which was due to the one-electron process of Fe(II)/Fe(III).

In the LB films of Zn-Bisterpy/PSS and Fe-Bisterpy/PSS, similar redox waves were recorded, with the peak potentials

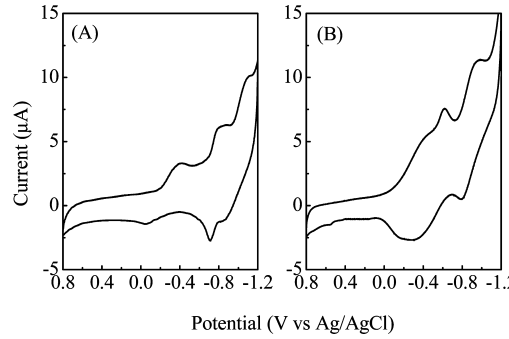

FIGURE 9. Cyclic voltammograms for (A) the Fe-Bisterpy complex and (B) the Fe-Bisterpy/PSS LB film in the 10 mmol/L KCl electrolyte solution at scan rate of 50 mV/s.

slightly shifted to lower positions, which may be attributed to an increase of film resistance. Also due to the film resistance, the potential difference became slightly larger in the LB films. These phenomena have often been observed in the organized thin films of electroactive compounds (26). Because of such a peak shift, the redox couple of Fe(II)/Fe(III) overlapped with that of the first couple of the ligand (Bisterpy^{2+} ↔ Bisterpy$^{\bullet+}$); therefore, a broad band was observed in the potential range of 0−0.6 V for the electrode modified by the LB film of Fe-Bisterpy/PSS (Figure 9B).

Electrochromic Properties. It has been revealed that the ligand Bisterpy showed a color change when it was reduced, as occurred for the viologen derivatives (27). During our experiments, we found that, although both the LB films of the pure ligand and its coordination polymers showed reversible redox behaviors and electrochromic properties, a clearer color change could be distinguished only for the LB films of Bisterpy/PSS and Zn(Cd)-Bisterpy/PSS, not for the LB film of Fe-Bisterpy/PSS, since it had an absorption band at around 550 nm.

Here, as an example, Figure 10A shows absorption spectra for the LB film of Bisterpy/PSS on the ITO electrode surface with and without an applied potential of −1.1 V vs Ag/AgCl. Because the ITO electrode used was not optically transparent at wavelengths below 350 nm, almost no ab-

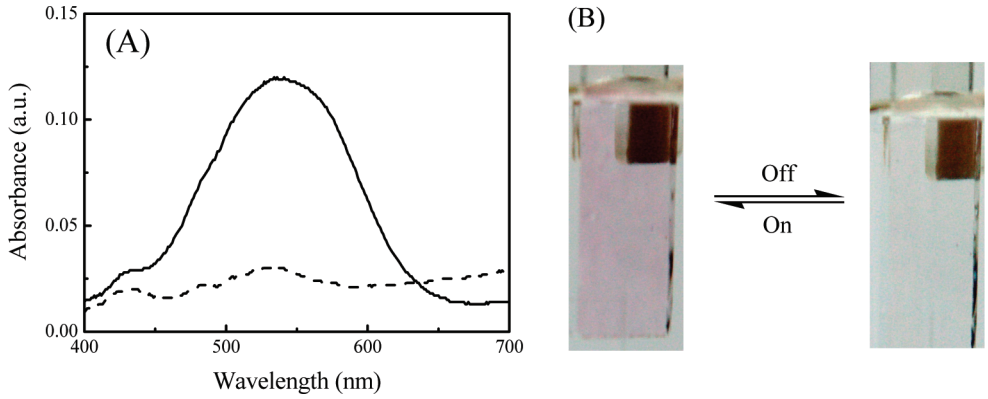

FIGURE 10. (A) Absorption spectra for Bisterpy/PSS LB films with (—) and without (- - -) an applied potential of −1.1 V vs Ag/AgCl. (B) Photos of Bisterpy/PSS LB films with (left) and without (right) the applied potential.

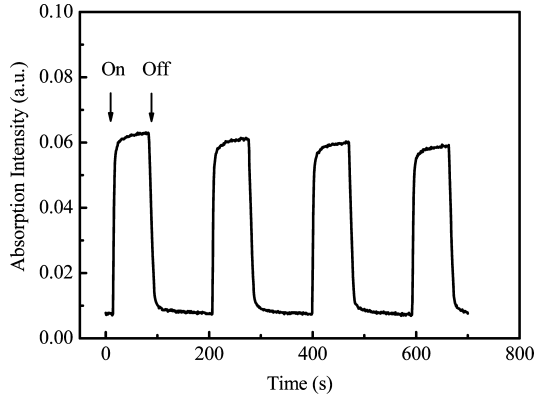

FIGURE 11. Plot of absorption intensity at 541 nm vs time for the Bisterpy/PSS LB film with or without an applied potential of −1.1 V vs Ag/AgCl.

sorption peaks were recorded for the LB film modified electrode without the applied potential. On the other hand, when a potential of −1.1 V was applied, a rather strong absorption band was recorded from 460 to 610 nm, with the maximum wavelength at 541 nm. This spectral change was accompanied by a color change for the ITO electrode, that is, from almost no color to a weak redness, the photos of which are given in Figure 10B.

To give more information on such an electrochromic response of the LB film modified electrode, we further measured a dynamic process for the absorption intensity with and without an applied potential of −1.1 V. The electrochromic response for the LB films of Bisterpy/PSS and M-Bisterpy/PSS modified ITO electrodes was carried out by recording the absorbance at 541 nm. As an example, Figure 11 shows the absorption intensity of the film at 541 nm as a function of time. This curve indicates a rapid increase of the absorbance upon an increase in potential, which nearly completely recovers when the applied potential is stopped. Both steps could be finished within an order of seconds with good reproducibility, which indicates that the electrochemical reduction of the Bisterpy ligand or M-Bisterpy complexes was a very quick process and vice versa.

As we have mentioned above, the present LB films showed quite strong stability and uniformity because each positively charged Bisterpy or M-Bisterpy layer was separated by another layer of negatively charged PSS. Such a film performance, together with such a quick and reversible color change accompanied by applied potential, makes it possible for the present LB films to be considered as potential materials for molecular switches and display devices.

CONCLUSIONS

We have demonstrated the assembly of metal-bisterpyridine coordination polyelectrolytes and their Langmuir–Blodgett films at air–water interfaces. Because of the coexisting anionic polymer, the as-prepared films had strong stability and good uniformity. Quasi-reversible redox behaviors were revealed for the film-modified electrodes, which corresponded to the electron transfer processes of either ligands or metal ions. A rapid and reversible color change of the films under applied potential or not suggest that the present molecular aggregates could be used as potential materials for the development of redox-based molecular switches and display devices. Moreover, it is suggested that the present methodology could provide a facile way to design and construct organized ultrathin films of functional polyelectrolyte hybrids at interfaces.

Acknowledgment. We are grateful to the National Science Foundation of China (Grant Nos. 20873030 and 20421303) and the Shanghai Leading Academic Discipline Project (Grant No. B108) for financial support.

Supporting Information Available: Figures giving additional plots and spectra of the materials studied in this paper. This material is available free of charge via the Internet at http://pubs.acs.org.

REFERENCES AND NOTES

(1) (a) Ye, B.-H.; Tong, M.-L.; Chen, X.-M. *Coord. Chem. Rev.* **2005**, *249*, 545–565. (b) South, C. R.; Burd, C.; Weck, M. *Acc. Chem. Res.* **2007**, *40*, 63–74. (c) Kaneko, W.; Ohba, M.; Kitagawa, S. *J. Am. Chem. Soc.* **2007**, *129*, 13706–13712.

(2) (a) Seki, K.; Mori, W. *J. Phys. Chem. B* **2002**, *106*, 1380–1385. (b) Ohashi, H.; Hiraoka, Y.; Yamaguchi, T. *Macromolecules* **2006**, *39*, 2614–2620. (c) Zhang, J. P.; Lin, Y. Y.; Zhang, W. X.; Chen, X. M. *J. Am. Chem. Soc.* **2005**, *127*, 14162–14163.

(3) (a) Han, J. W.; Hill, C. L. *J. Am. Chem. Soc.* **2007**, *129*, 15094–15095. (b) Horike, S.; Matsuda, R.; Tanaka, D.; Mizuno, M.; Endo, K.; Kitagawa, S. *J. Am. Chem. Soc.* **2006**, *128*, 4222–4223. (c) Hasegawa, S.; Horike, S.; Matsuda, R.; Furukawa, S.; Mochizuki, K.; Kinoshita, Y.; Kitagawa, S. *J. Am. Chem. Soc.* **2007**, *129*, 2607–2614.

(4) Kitagawa, S.; Kitaura, R.; Noro, S. *Angew. Chem., Int. Ed.* **2004**, *43*, 2334–2375.

(5) (a) Constable, E. C.; Fromm, K. M. *Coord. Chem. Rev.* **2008**, *252*, 842–855. (b) Fromm, K. M. *Coord. Chem. Rev.* **2008**, *252*, 856–885.
(6) (a) Reger, D. L.; Watson, R. D.; Gardinier, J. R.; Smith, M. D. *Inorg. Chem.* **2004**, *43*, 6609–6619. (b) Zhang, H. M.; Zhao, W.; Xie, Z. X.; Long, L. S.; Mao, B. W.; Xu, X.; Zheng, L. S. *J. Phys. Chem. C* **2007**, *111*, 7570–7573.
(7) (a) Dobrawa, R.; Lysetska, M.; Ballester, P.; Grüne, M.; Würthner, F. *Macromolecules* **2005**, *38*, 1315–1325. (b) Teo, T.-L.; Vetrichelvan, M.; Lai, Y.-H. *Org. Lett.* **2003**, *5*, 4207–4210.
(8) (a) Tokuhisa, H.; Kanesato, M. *Langmuir* **2005**, *21*, 9728–9732. (b) Byrd, H.; Holloway, C. E.; Pogne, J.; Kircus, S.; Advincula, R. C.; Knoll, W. *Langmuir* **2000**, *16*, 10322–10328. (c) Shekhah, O.; Wang, H.; Strunskus, T.; Cyganik, P.; Zacher, R.; Fischer, R.; Wöll, C. *Langmuir* **2007**, *23*, 7440–7442.
(9) (a) Qian, D. J.; Wakayama, T.; Nakamura, C.; Miyake, J. *J. Phys. Chem. B* **2003**, *107*, 3333–3335. (b) Liu, B.; Qian, D. J.; Huang, H.-X.; Wakayama, T.; Hara, S.; Huang, W.; Nakamura, C.; Miyake, J. *Langmuir* **2005**, *21*, 5079–5084. (c) Liu, B.; Qian, D. J.; Chen, M.; Wakayama, T.; Nakamura, C.; Miyake, J. *Chem. Commun.* **2006**, 3175–3177. (d) Liu, B.; Chen, M.; Nakamura, C.; Miyake, J.; Qian, D. J. *New J. Chem.* **2007**, *31*, 1007–1011. (e) Zhang, C. F.; Chen, M.; Nakamura, C.; Miyake, J.; Qian, D. J. *Langmuir* **2008**, *24*, 13490–13495.
(10) (a) Chen, X.; Lenhert, S.; Hirtz, M.; Lu, N.; Fuchs, H.; Chi, L. *Acc. Chem. Res.* **2007**, *40*, 393–401. (b) Jiang, J. Z.; Ng, D. K. P. *Acc. Chem. Res.* **2009**, *42*, 79–88.
(11) (a) Constable, E. C.; Dunphy, E. L.; Housecroft, C. E.; Kylberg, W.; Neuburger, M.; Schaffner, S.; Schofield, E. R.; Smith, C. B. *Chem. Eur. J.* **2006**, *12*, 4600–4610. (b) Constable, E. C.; Housecroft, C. E.; Neuburger, M.; Schaffner, S.; Schaper, F. *Inorg. Chem. Commun.* **2006**, *9*, 616–619. (c) Hou, L.; Li, D.; Shi, W.-J.; Yin, Y.-G.; Ng, S. W. *Inorg. Chem.* **2005**, *44*, 7825–7832.
(12) (a) Kelch, S.; Rehahn, M. *Macromolecules* **1999**, *32*, 5818–5828. (b) Duprez, V.; Biancardo, M.; Spanggaard, H.; Krebs, F. C. *Macromolecules* **2005**, *38*, 10436–10448.
(13) (a) Goodall, W.; Williams, J. A. G. *Dalton Trans.* **2000**, 2893–2895. (b) Davidson, G. J. E.; Loeb, S. J. *Dalton Trans.* **2003**, 4319–4323. (c) Constable, E. C.; Housecroft, C. E.; Neuburger, M.; Philips, D.; Raithby, P. R.; Schofield, E.; Sparr, E.; Tocher, D. A.; Zehnder, M.; Zimmermann, Y. *Dalton Trans.* **2000**, 2219–2228.
(14) Kurth, D. G.; Lopez, J. P.; Dong, W. F. *Chem. Commun.* **2005**, 2119–2121.
(15) (a) Han, F. S.; Higuchi, M.; Ikeda, T.; Negishi, Y.; Tsukuda, T.; Kurth, D. G. *J. Mater. Chem.* **2008**, *18*, 4555–4560. (b) Han, F. S.; Higuchi, M.; Kurth, D. G. *Tetrahedron* **2008**, *64*, 9108–9116. (c) Han, F. S.; Higuchi, M.; Kurth, D. G. *J. Am. Chem. Soc.* **2008**, *130*, 2073–2081.
(16) Zhang, C. F.; Liu, A.; Chen, M.; Qian, D. J. *Chem. Lett.* **2008**, *37*, 444–445.
(17) (a) Sagara, T.; Kaba, N.; Komatsu, M.; Uchida, M.; Nakashima, N. *Electrochim. Acta* **1998**, *43*, 2183–2193. (b) Tanaka, Y.; Sagara, T. *J. Electroanal. Chem.* **2008**, *619*, 65–74. (c) Sagara, T.; Miuchi, K. *J. Electroanal. Chem.* **2004**, *567*, 193–202.
(18) Noda, K.; Zorin, N. A.; Nakamura, C.; Miyake, M.; Gogotov, I. N.; Asada, Y.; Akutsu, H.; Miyake, J. *Thin Solid Films* **1998**, *327–329*, 639–642.
(19) (a) Wang, Y.; Stedronsky, E.; Regen, S. L. *Langmuir* **2008**, *24*, 6279–6284. (b) McCullough, D. H., III; Grygorash, R.; Regen, S. L. *Langmuir* **2007**, *23*, 9606–9610. (c) Salomäki, M.; Kankare, J. *Macromolecules* **2008**, *41*, 4423–4428.
(20) Zhang, C. F.; Huang, H. X.; Liu, B.; Chen, M.; Qian, D. J. *J. Lumin.* **2008**, *128*, 469–475.
(21) (a) Constable, E. C.; Housecroft, C. E.; Neuburger, M.; Schaffner, S.; Schaper, F. *Inorg. Chem. Commun.* **2006**, *9*, 434–436. (b) Meng, X.; Song, Y.; Hou, H.; Han, H.; Xiao, B.; Fan, Y.; Zhu, Y. *Inorg. Chem.* **2004**, *43*, 3528–3536.
(22) (a) Qian, D. J.; Nakamura, C.; Miyake, J. *Langmuir* **2000**, *16*, 9615–9619. (b) Liu, B.; Chen, H. T.; Qian, D. J. *Prog. Chem.* **2007**, *19*, 872–877. (c) Liu, B.; Huang, H. X.; Zhang, C. F.; Chen, M.; Qian, D. J. *Thin Solid Films* **2008**, *516*, 2144–2150.
(23) Since the binding energy of Cd(3d) was close to that of the N atom, it was difficult to calculate the elemental ratio N:Cd. It was also found that the metal ions could be adsorbed by the monolayers; thus, it is better to wash the deposited LB films with pure water before the XPS measurements.
(24) (a) Sharma, C. V. K.; Broker, G. A.; Huddleston, J. G.; Baldwin, J. W.; Metzger, R. M.; Roger, R. D. *J. Am. Chem. Soc.* **1999**, *121*, 1137–1144. (b) Beves, J. E.; Bray, D. J.; Clegg, J. K.; Constable, E. C.; Housecroft, C. E.; Jolliffe, K. A.; Kepert, C. J.; Lindoy, L. F.; Neuburger, M.; Price, D. J.; Schaffner, S.; Schaper, F. *Inorg. Chim. Acta* **2008**, *361*, 2582–2590.
(25) (a) Zhang, C. F.; Chen, M.; Nakamura, C.; Miyake, J.; Qian, D. J. *Langmuir* **2008**, *24*, 13490–13495. (b) Liu, A. R.; Wang, X.; Nakamura, C.; Miyake, J.; Zorin, N. A.; Qian, D. J. *J. Phys. Chem. C* **2008**, *112*, 1582–1588.
(26) (a) Lee, N. S.; Shin, H. K.; Qian, D. J.; Kwon, Y. S. *Jpn. J. Appl. Phys.* **2007**, *46*, 2745–2748. (b) Lee, N. S.; Shin, H. K.; Qian, D. J.; Kwon, Y. S. *Thin Solid Films* **2007**, *515*, 5163–5166.
(27) (a) Han, F. S.; Higuchi, M.; Akasaka, Y.; Otsuka, Y.; Kurth, D. G. *Thin Solid Films* **2008**, *516*, 2469–2473. (b) Huang, H. X.; Qian, D. J.; Nakamura, N.; Nakamura, C.; Wakayama, T.; Miyake, J. *Electrochim. Acta* **2004**, *49*, 1491–1498.

AM900135G